TECHNICAL REPORT NO. 5

Spin-Orbital Electronegativity, the Xα Method, and Reactivity at Transition-Metal Interfaces
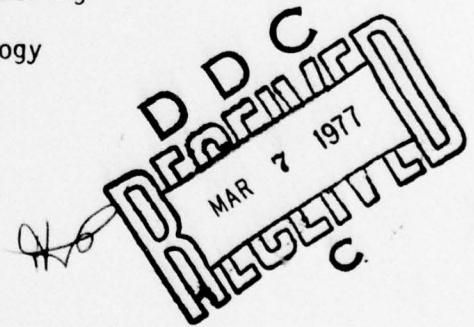
by

K. H. Johnson

Department of Materials Science and Engineering

and

Center for Materials Science and Engineering

Massachusetts Institute of Technology

Cambridge, Massachusetts 02139

February 28, 1977

2

REPORT DOCUMENTATION PAGE		READ INSTRUCTIONS BEFORE COMPLETING FORM
1. REPORT NUMBER TR - 5	2. GOVT ACCESSION NO.	3. RECIPIENT'S CATALOG NUMBER
4. TITLE (and Subtitle) SPIN-ORBITAL ELECTRONEGATIVITY, THE Xα METHOD, AND REACTIVITY AT TRANSITION-METAL INTERFACES.		5. TYPE OF REPORT & PERIOD COVERED Interim rept.
		6. PERFORMING ORG. REPORT NUMBER
7. AUTHOR(s) K. H. Johnson		8. CONTRACT OR GRANT NUMBER(s) N00014-75-C-0970
9. PERFORMING ORGANIZATION NAME AND ADDRESS Department of Materials Science and Engineering Massachusetts Institute of Technology Cambridge, Massachusetts 02139		10. PROGRAM ELEMENT, PROJECT, TASK AREA & WORK UNIT NUMBERS Task No. NR 056-596
11. CONTROLLING OFFICE NAME AND ADDRESS Office of Naval Research Department of the Navy Arlington, Virginia 22217		12. REPORT DATE February 28, 1977
		13. NUMBER OF PAGES
14. MONITORING AGENCY NAME & ADDRESS(if different from Controlling Office)		15. SECURITY CLASS. (of this report) Unclassified
		15a. DECLASSIFICATION/DOWNGRADING SCHEDULE

16. DISTRIBUTION STATEMENT (of this Report)

Approved for public release; distribution unlimited.

17. DISTRIBUTION STATEMENT (of the abstract entered in Block 20, if different from Report)

18. SUPPLEMENTARY NOTES

19. KEY WORDS (Continue on reverse side if necessary and identify by block number)

spin-orbital electronegativity; Xα method; reactivity; transition-metal interfaces

409 463

20. ABSTRACT (Continue on reverse side if necessary and identify by block number)

It is shown that the concept of electronegativity, originally viewed as a virtually constant characteristic of an atom, can be generalized to the individual molecular orbitals of aggregates of atoms, utilizing the self-consistent-field X-alpha (SCF-Xα) density-functional representation of molecular-orbital theory in conjunction with the definition of orbital electronegativity proposed by Hinze et al. This generalization allows for the dependence of electronegativity on the detailed electronic structure of a

next page

SECURITY CLASSIFICATION OF THIS PAGE(When Data Entered)

cont. →

20.

group of atoms as a function of its composition, geometry, and local chemical environment. In transition metals and transition-metal coordination complexes, where local magnetic spin polarization of electrons is important, the concept of orbital electronegativity can be further generalized to the individual spin-orbitals. By viewing a transition-metal surface, cluster, or coordination complex as providing orbital or spin-orbital pathways for electrons to effectively flow between reactants, where such flow directly between reactants in the gas phase is forbidden by orbital-symmetry restrictions or unfavorable electronegativity differences, orbital or spin-orbital electronegativity can be used in conjunction with SCF-Xα calculations for   X-alpha representative clusters and complexes as an approximate index of heterogeneous or homogeneous reactivity. Recent applications of this concept to a number of problems associated with reactivity at transition-metal interfaces are reviewed, including:

(1) The dissociation and reactivity of hydrogen at low-coordination transition-metal sites;
(2) The interaction of atomic hydrogen with transition-metal interfaces; and
(3) The surface reactivity of iron.

SECURITY CLASSIFICATION OF THIS PAGE(When Data Entered)

I. INTRODUCTION

One of the major goals of surface chemistry and physics is to elucidate the fundamental nature of chemical reactivity at surfaces and interfaces. In particular, transition metals and their alloys have been a focus of attention in regard to the generally high surface reactivity of these materials, in both their crystalline form and in the form of small particles and clusters which constitute the active centers of supported heterogeneous catalysts. Molecular transition-metal coordination complexes are often centers of homogeneous catalysis.

In characterizing surface reactivity and heterogeneous catalytic activity, it is customary for one to distinguish between those reactions which are structure-sensitive or "demanding" and those reactions which are structure-insensitive or "facile" [1] Most heterogeneous reactions are, in fact, facile. The relatively few which are demanding usually vary in activity by no more than one order of magnitude over a range of surface structures, for fixed average surface composition. On the other hand, heterogeneous reactivity, facile or demanding, may vary by several orders of magnitude with changes in surface composition. For example, among the Group-VIII transition metals, osmium, iridium, and platinum, the catalytic activity for ethane hydrogenolysis, a demanding reaction, varies by seven orders of magnitude [2]. As another striking example, the alloying of only five atomic percent of copper with nickel reduces the catalytic activity of the latter metal for ethane hydrogenolysis by three orders of magnitude, attributed largely to surface segregation of copper [2].

The dominance of surface composition over surface geometry in determining heterogeneous reactivity suggests that one might look for electronic indices of surface reactivity, dependent on surface electronic structure, which would be an approximate gauge of the relative activities and selectivities of surfaces of different composition, with respect to specific reactants.

The establishment of such indices could ultimately serve as a guide in the systematic optimization of surface activity and selectivity through alloying or chemical modification. Since surface electronic structure can vary with morphology, e.g., surface "roughness" or particle dispersion, the structure sensitivity of certain reactions, although more subtle than composition sensitivity, should also be within the scope of such electronic indices.

During the past two years, we have been investigating the electronic structures of clusters and coordination complexes which are theoretical models for active sites, chemisorption, and reaction intermediates at transition-metal interfaces, utilizing the self-consistent-field X-alpha scattered-wave (SCF-Xα-SW) density-functional approach to molecular-orbital theory [3]. The assumptions underlying this approach are that chemisorption and heterogeneous reactivity on the active sites of transition-metal clusters and surfaces are governed by essentially the same types of electronic factors which determine the metal-ligand bonding and homogeneous reactivity of isolated transition-metal coordination complexes. The initial phases of this work are described in detail in two recent articles [4,5].

II. SPIN-ORBITAL ELECTRONEGATIVITY AND THE SCF-Xα METHOD

A recent outgrowth of these theoretical studies is the establishment of "spin-orbital electronegativity," defined by the SCF-Xα spin-orbital energies for representative surface clusters and coordination complexes, as a reactivity index of the type described in the preceding section. The concept of spin-orbital electronegativity is derived from the fact that the orbital energy eigenvalues in the SCF-Xα theory are rigorously equal to first derivatives of the total energy with respect to orbital occupation number [3,6], i.e.,

$$\epsilon_{iX\alpha} = \partial <E_{X\alpha}>/\partial n_i \qquad (1)$$

These quantities should not be identified with the orbital energies defined
in conventional Hartree-Fock theory [6], namely, as the differences

$$\epsilon_{iHF} = <E_{HF}(n_i=1)> - <E_{HF}(n_i=0)> \qquad (2)$$

between single-determinant total energies calculated when the ith orbital is
occupied and when it is empty (fixing the remaining occupied orbitals).
The $X\alpha$ orbital energies defined in Eq. (1) correspond closely to the orbital
electronegativities

$$X_i = \partial E/\partial n_i \qquad (3)$$

defined by Hinze et al. [7] as a generalization of Mulliken's [8] definition
of electronegativity

$$X_M = \frac{1}{2}(I+A), \qquad (4)$$

where I is the ionization potential and A is the electron affinity of a
chemically bonded atom in its valence state.

This generalization, its relationship to SCF-$X\alpha$ theory, and ultimately
its use as an index of reactivity can be understood better if one recalls
that electronegativity, as originally defined by Pauling [9], is a measure
of the power of a chemically bonded atom to attract electrons to itself.
Pauling believed that electronegativity is a virtually constant atomic
property, even for different valence states of the same element, and established
a scale of electronegativities for the elements based on the empirical bond
energies of heteronuclear diatomic molecules. Despite the arbitrariness of
this scale and the uncertainties in the thermochemical data on which it is
based, a wide variety of chemical phenomena have been reasonably explained
through the use of Pauling's electronegativity scale.

Pauling's concept of electronegativity as a fixed atomic characteristic
is somewhat more restrictive than Mulliken's definition of electronegativity
in terms of the valence-state ionization potential I and electron affinity A,

since one does not expect that I and A or their average should be constant for different valence or oxidation states of a chemically bonded atom. Thus while Mulliken's electronegativity scale, in its simplest form, can be adjusted to agree reasonably well with Pauling's scale, element by element, Mulliken's concept is more satisfying from a theoretical point of view and allows, in principle, for the dependence of electronegativity on the chemical environment of an atom.

Since I and A are quantities related respectively to the removal of an electron from the highest occupied atomic orbital and the addition of an electron to the lowest unoccupied orbital, it might be expected that Mulliken's concept of electronegativity could be further generalized to all the orbitals of a chemically bonded atom and indeed to the molecular orbitals of an aggregate of atoms. Thus one is led to the concept of orbital electronegativity as a measure of the power of a chemically bonded atom or molecular aggregate to attract an electron to a particular atomic or molecular orbital. The mathematical definition of orbital electronegativity as the first derivative of the total energy with respect to occupation number, given in Eq. (3) in the form suggested by Hinze et al. [7], is consistent with the above conceptual definition. Implicit in Eq. (3) are the two assumptions: (a) that the occupation numbers n_i may have both integral and non-integral values, and (b) that once assumption (a) is made, then the total energy E is a continuous and differentiable function of the occupation numbers.

The occupation numbers n_i and statistical total energy $E_{X\alpha}$ defined in the $X\alpha$ density-functional self-consistent-field theory fulfill both of the above conditions, so that one can uniquely identify the SCF-$X\alpha$ electronic energy eigenvalues $\varepsilon_{iX\alpha}$ of an atom, molecule, or cluster, as given in expression (1), with the orbital electronegativities defined in Eq. (3).

In the limit where the total energy is a quadratic (parabolic) function of the occupation number, the orbital electronegativity reduces exactly to Mulliken's definition of electronegativity given in Eq. (4) [7]. This follows from a simple geometric theorem which relates the slope of the chord of a parabola to the slope of the parabola at its midpoint. The same type of argument applied to SCF-Xα orbitals leads to Slater's transition-state concept [6], whereby one determines I or A for an atom, molecule, or cluster by subtracting or adding one-half a unit of valence orbital electronic charge and then calculating self-consistently the energy of the relaxed orbital. While these relaxed transition-state energies can be individually identified with the corresponding orbital ionization potentials or electron affinities, the unrelaxed ground-state SCF-Xα orbital energies $\varepsilon_{iX\alpha}$ define a set of orbital electronegativities. Thus the relative positions of the SCF-Xα electronic energy levels for a system of interacting or reacting atoms, molecules, or clusters are a measure of the orbital electronegativity and chemical-potential differences between the various reactants.

In those systems where magnetic spin polarization is important, one may use the spin-unrestricted version of the SCF-Xα method to calculate different orbitals for different spins, leading to spin-polarized energy levels $\varepsilon_{iX\alpha}\!\uparrow$ and $\varepsilon_{iX\alpha}\!\downarrow$ [3,6]. If these spin-dependent orbital energies are identified with orbital electronegativities, then one is automatically led to the concept of spin-orbital electronegativity as a measure of the power of an atom or molecular aggregate to attract an electron to a particular atomic or molecular spin orbital. For example, the spin dependence of orbital electronegativity is central to understanding the surface reactivity of iron (see Section V).

To understand the relationship between spin-orbital electronegativity, as represented by the SCF-Xα spin-orbital energy levels of representative surface clusters and reactants, and surface reactivity, it is helpful to

recall the following concept originally introduced by Fukui [10]. For a concerted chemical reaction to occur with reasonable activation energy, electrons must be able to flow between the reactants from occupied orbitals into unoccupied orbitals with which they have net positive overlap, as the reactants move along the reaction coordinate. Overlap and electron flow will be ensured if the pertinent reactant orbitals have the following characteristics: (a) the same symmetry (i.e., orbital symmetry conservation as originally proposed by Woodward and Hoffmann [11]), and (b) equal or nearly equal orbital electronegativities. In the limit where electron flow between reactants is simply from the highest occupied molecular orbital (HOMO) to the lowest unoccupied molecular orbital (LUMO), condition (b) is equivalent to the requirement that the energy gap between HOMO and LUMO be as small as possible [12].

Where direct electron flow between reactants is forbidden by orbital symmetry restrictions or unfavorable orbital electronegativity differences (implying a large activation energy), a surface can heterogeneously catalyze the reaction by providing a pathway for such electron flow, e.g., through chemisorption via spatially directed or hybridized d-orbitals in the case of a transition-metal surface. Similar arguments are applicable to isolated transition-metal coordination complexes which homogeneously catalyze electron flow between reactants through bonding and exchange of ligands.

III. THE DISSOCIATION AND REACTIVITY OF HYDROGEN
AT LOW-COORDINATION TRANSITION-METAL SITES

It is well known, for example, that certain "coordinatively unsaturated" transition-metal complexes in solution can homogeneously catalyze chemical reactions [13], while it has long been suspected that low-coordination sites on transition-metal surfaces and supported transition-metal clusters are

centers of heterogeneous reactivity [14,15]. In this section, it will be shown that the SCF-Xα electronic structure of such complexes, in conjunction with the concept of orbital electronegativity, is consistent with their reactivity and is suggestive of how low-coordination sites on transition-metal surfaces can act as centers of reactivity. The dissociation and reactivity of H_2 is considered as an illustrative example.

As a working model, we consider a Group-VIII transition-metal atom (M) dihedrally coordinated by ligands (L), yielding the coordinatively unsaturated L_2M complex illustrated at the top of Fig. 1. This model has the advantage that it can realistically represent transition-metal complexes of the type (e.g., M = Pt, Ir, Rh; L = Ph_3P = triphenylphosphine) which dissociatively bind and homogeneously catalyze reactions of H_2 [13], and it can simulate low-coordination sites (e.g., "corner atoms") of faceted transition-metal clusters or stepped transition-metal surfaces which dissociatively chemisorb and heterogeneously catalyze reactions of H_2 [14,15]. In the latter systems, the ligand (L) is also a metal atom, either of the same species as the transition metal (M), or of a different species in the case of an alloy surface or bimetallic cluster.

Molecular-orbital calculations have been carried out for L_2M and L_2MH_2 complexes by the SCF-Xα-SW method as a function of metal species (M = Pt, Ir), ligand species (L = phosphine, Pt), and molecular geometry. The resulting orbital energies for M = Pt, L = phosphine, and geometry characteristic of the platinum-phosphine complexes described in Ref. 13 are shown in Fig. 1. Also shown, for comparison, are the SCF-Xα orbital energies for the isolated metal, ligand, and hydrogen molecule at the free-molecule internuclear distance 0.74 $\overset{\circ}{A}$ (H_2) and internuclear distance 2.8 $\overset{\circ}{A}$ (H_2*) characteristic of the partially dissociated ("dihydride") configuration of H_2 in the L_2MH_2 complex.

The SCF-Xα orbital energy eigenvalues shown in Fig. 1 can be rigorously

identified with orbital electronegativities which are a measure of the relative average electron donor-acceptor character of the individual orbitals, as described in the preceding section. Thus the fact that the isolated ligand energy level, which corresponds to a phosphine "lone-pair" orbital, nearly coincides with the d-orbital energy level of the isolated Pt atom (neglecting relativistic shifts) implies a predominantly covalent L-Pt(5d) interaction similar to that expected for a direct Pt(5d)-Pt(5d) interaction. In this respect, the effect of coordinatively unsaturated phosphine ligands on the electronic structure of a platinum atom is expected to be similar to that of embedding a Pt atom in a low-coordination Pt environment, such as that provided by a surface or cluster.

The ligand-metal interaction in the L_2M complex leads to the bonding orbital energies labeled L-M(d_{yz}) and L-M(d_{z^2}) in Fig. 1, and to the antibonding orbital energies labeled M(d_{z^2})-L*, M(d_{yz})-L*, and M(s)-L*, of which M(d_{yz})-L* is the highest occupied energy level in the ground state of the complex. A simple interpretation of the position of the latter energy level is that the strong ligand-field repulsion of the metal d-orbital pointed on the ligand directions (the d_{yz} orbital for the chosen coordinate system) raises the energy level of this orbital, reduces the corresponding orbital electronegativity, and mixes in significant antibonding ligand character. The d_{z^2} orbital is also subject to some antibonding ligand-field repulsion, whereas the $d_{x^2-y^2}$, d_{xz}, and d_{xy} orbitals remain essentially nonbonding.

When platinum atoms are substituted for the phosphine ligands, the electronic structure reduces to the manifold of bonding, nonbonding, and antibonding d-orbital energy levels (the "d-band") characteristic of a small platinum cluster [4]. In this case, the M(d_{yz})-L* (L = M) antibonding orbital may be interpreted as the analogue of a localized "surface state" which is split off from the top of the d-band.

The most important result of the strong ligand-metal antibonding component is to bring the $M(d_{yz})$-L* orbital, the highest occupied orbital, closer in energy and electronegativity (as compared with the isolated Pt atom) to the empty antibonding σ_u orbital of the H_2 molecule. This facilitates overlap and electron flow between the $M(d_{yz})$-L* and σ_u orbitals, which are symmetry conserving [11], thereby promoting dissociation of H_2. The partially dissociated molecule (H_2*), characterized by σ_g and σ_u orbital energies approaching the SCF-Xα 1s orbital energy of a free hydrogen atom (see Fig. 1), can bind or "chemisorb" in a dihydride configuration to the coordinatively unsaturated metal site. This is revealed by the L_2MH_2 molecular-orbital energies shown in Fig. 1 and the corresponding orbital wavefunction contour maps shown in Fig. 2. The $2b_2$ orbital, for example, results from overlap and electron flow between the $M(d_{yz})$-L* orbital and the H_2 σ_u orbital. The dihydride configuration is further stabilized by the "butterfly-like" $1a_1$ and $2a_1$ orbitals shown in Fig. 2, formed from the overlap of the equatorial parts of the L-$M(d_{z^2})$ and $M(d_{z^2})$-L* orbitals with the H(1s) (or H_2* σ_g) orbitals. Note that the $M(d_{z^2})$ lobe pointed along the z-direction acts as a repulsive barrier which helps to keep the H atoms apart. These dihydride bonding orbitals are offset somewhat by the $4a_1$ and $3a_1$ orbitals resulting respectively from the antibonding interaction of the L-$M(d_{z^2})$ and $M(d_{x^2-y^2})$ orbitals with the H_2* σ_g orbital, as is evident in the $4a_1$ orbital contour map shown in Fig. 2. There is negligible contribution of the M(s) orbital component in the binding of hydrogen to these platinum and iridium complexes. This is consistent with the finding, based on SCF-Xα cluster calculations [16] and photoemission studies [17], that the metal d-orbitals are almost exclusively responsible for the chemisorption of hydrogen on second- and third-row transition metals such as palladium and platinum, whereas significant metal s,d-hybridization (with the s-orbital component dominant) is involved in

hydrogen chemisorption on first-row transition metals such as nickel. Since the deuterium molecule (D_2) is chemically identical to the hydrogen molecule (H_2), all the results described above for the dissociation of H_2 at a low-coordination transition-metal site apply equally well for the dissociation of D_2 at such a site.

The above described electronic structure of the L_2MH_2 (or L_2MD_2) coordination complex leads to possible explanations of the observed homogeneous and heterogeneous catalytic reactivity of H_2 (or D_2). For example, the near cancellation of the contributions of the bonding ($1a_1$, $2a_1$) orbitals and antibonding ($3a_1$, $4a_1$) orbitals to metal-hydrogen bond strength, leaving the dissociative $2b_2$ bonding orbital dominant, explains the relatively weak, reversible binding of H_2 (or D_2) to such complexes and their ability to activate H_2-D_2 exchange [13]. Since such a complex is also a good model for H_2 (or D_2) dissociation at the corner atoms of a platinum surface step, the results suggest why atomic steps on platinum surfaces are essential in dissociating H_2 and D_2 and in activating H_2-D_2 exchange [14].

The electronic structure of the L_2MH_2 complex also suggests a possible reaction path for the hydrogenation of unsaturated hydrocarbons at low-coordination transition-metal sites. The $4a_1$ orbital, which defines the Fermi energy of the site, is closely matched in symmetry, energy, and electronegativity to the π orbitals of hydrocarbons such as acetylene (C_2H_2) and ethylene (C_2H_4). When the $4a_1$ orbital, which is an antibonding mixture of L-M(d_{z^2}) and H_2^* σ_g orbital character, is only partially occupied (as is the case for M = Ir, Rh), it offers a pathway for electron flow from a C_2H_2 (or C_2H_4) π orbital to the dissociatively "chemisorbed" hydrogen. Electron flow directly between C_2H_2 (or C_2H_4) and H_2 in the gas phase via the filled π and σ_g orbitals is forbidden by the Pauli exclusion principle, whereas electron flow directly between the π orbital and empty σ_u orbital is

forbidden by orbital symmetry [11]. Because the $4a_1$ orbital of L_2MH_2 is antibonding between the L_2M site and H_2, while bonding between H_2 and C_2H_2 (or C_2H_4), the net result of electron flow between a π orbital and the $4a_1$ orbital is the breaking of a C-C π bond, the formation of two new C-H bonds, and the expulsion of the hydrogenated species C_2H_4 (or C_2H_6), as suggested by the reaction path shown in Fig. 3. Also shown is a contour map for the $4a_1$ orbital of the $L_2MH_2C_2H_2$ reaction intermediate (the third step of the proposed reaction path) formed as a result of the interaction of acetylene with the L_2MH_2 complex. The incipient formation of C-H bonds via the overlap of the C-C π orbital with the antibonding metal-dihydride orbital and the resulting ethylene-like configuration are clearly visible in this map. It is important to note that the concerted reaction path indicated in Fig. 3 is not the conventional one for hydrogenation on ideal transition-metal surfaces, where it is usually assumed that chemisorption of acetylene or ethylene on one or two metal sites is the precursor to combining with hydrogen chemisorbed on neighboring sites. Nonconcerted reaction paths in which both reactants are coordinated to the same metal site are also possible and indeed have been argued to be favored kinetically in certain homogeneous reactions [18]. Alternative reaction paths at low-coordination transition-metal sites are currently under investigation in conjunction with theoretical studies of the reactivity of $IrCl(CO)(Ph_3P)_2$ (Vaska's complex) [19].

In this section, we have attempted to show that a detailed theoretical study of the electronic structure of well characterized coordinatively unsaturated transition-metal complexes and their interactions with H_2 can not only lead to an understanding of their homogeneous reactivity but can also serve as a model for the dissociative chemisorption and heterogeneous reactivity of H_2 on low-coordination transition-metal surface sites, where definitive structural information is lacking. There are many useful analogies to be made between molecular transition-metal coordination complexes and

surface-adsorbate interactions [20,21]. Such analogies are probably not fortuitous. They should be sought after and the common basis of understanding elucidated.

In concluding this section, it is important to compare the present theoretical approach to surface reactivity, based on molecular-orbital indices, with other theoretical approaches to this problem and to chemical reactivity in general. In the applications of traditional methods of quantum chemistry (e.g., Hartree-Fock, Configuration-Interaction, Valence-Bond, etc.) to reaction kinetics and thermochemistry, one usually focuses directly on the calculation of total energies, total-energy differences, and "potential surfaces" for the reactants. This is generally a computationally difficult and costly process to carry out over the various possible reaction paths, even for the simplest reactions. To appreciate the magnitude of this problem, one need only consider the recent status of the quantitative first-principles determination of the kinetics of one of the simplest gas-phase chemical reactions, namely, hydrogen-deuterium exchange, $H_2 + D \rightarrow HD + H$ [22]. This situation hardly makes one confident in the efficacy of quantum theory to "predict" the path or kinetics of surface-activated reactions on the basis of potential-surface computations. Even if one carries out total energy calculations for only a few representative molecular configurations, rather than for the entire potential surface, there is still the uncertainty associated with the direct subtraction of two total energies, which are usually large numbers, to obtain a relatively small energy difference of chemical significance.

The theoretical approach described in this paper, while not a substitute for ab initio potential-surface calculations, circumvents many of the difficulties associated with the latter approach. By placing emphasis on the determination of molecular-orbital indices of reactivity, rather than

total energies, for realistic transition-metal coordination complexes and clusters simulating local bulk and surface configurations, one retains the molecular-orbital picture which chemists have traditionally used and makes contact with the band-structure concept of solid-state and surface physics.

IV. THE INTERACTION OF ATOMIC HYDROGEN WITH TRANSITION-METAL INTERFACES

The interaction of hydrogen with Group-VIII transition metals such as Ni, Pd, and Pt is of fundamental importance in the understanding of (1) the dissociative chemisorption and reactivity of hydrogen on the surfaces of these metals [23], (2) the catalytic activity of small particles and clusters of these metals [15], and (3) the solubility of atomic hydrogen in these metals [24]. In a previous paper [4], it has been shown that the electronic structures of small globular Cu, Ni, Pd, and Pt clusters, as calculated by the SCF-Xα-SW method, exhibit most of the characteristics of the corresponding bulk crystalline band structures, while having additional features corresponding to the finite cluster size and "surface" atoms. In the preceding section, it has been shown that low-coordination transition-metal sites, such as those of a cluster or "stepped" surface, have local features of electronic structure which explain why such sites activate H_2 dissociation and catalyze H_2-D_2 exchange [14].

In the present section, we describe the results of SCF-Xα-SW studies for the electronic structure of four-atom tetrahedral Ni, Pd, and Pt clusters containing atomic hydrogen, carried out in collaboration with R. P. Messmer, D. R. Salahub, and C. Y. Yang. This work includes the first application of the relativistic Xα-SW formalism developed by Yang and Rabii [25] to metal clusters. The cluster configurations chosen for study have the advantage that they are large enough to represent the local effects on electronic band structure of embedding dissociated hydrogen atoms in a surface or bulk interstitial environment, yet small enough to permit the resolution of

individual metal-hydrogen bonding orbitals. As will be shown, the results
are in good agreement with photoemission spectra for hydrogen chemisorbed
on the (111) surfaces of crystalline Ni, Pd, and Pt [17], strongly suggesting
that the hydrogen atoms, as a result of their small size, might
penetrate the (111) surface planes and become embedded in the tetrahedral
interstices of the substrate. Moreover, the computed electronic structures,
in conjunction with the concept of orbital electronegativity, suggest that
in those metals where hydrogen solubility is high [24], absorption and
chemisorption are closely linked and can be described by essentially identical
theoretical models. This is supported by the observation that the photo-
emission spectrum for hydrogen dissolved in bulk palladium [26] is very
similar to that for hydrogen chemisorbed on palladium [17].

Molecular-orbital calculations were carried out for the representative
nickel, palladium, and platinum clusters using both the standard nonrela-
tivistic version of the SCF-$X\alpha$-SW method and the recently developed rela-
tivistic version [25], constraining metal-metal internuclear distances to
be equal to those for the corresponding crystalline metals. The resulting
relativistic orbital energies for the tetrahedral clusters with and without
interstitial atomic hydrogen are shown in Fig. 4. Also shown, for comparison,
is the SCF-$X\alpha$ 1s-orbital energy for the isolated hydrogen atom. The elec-
tronic energy levels are labeled according to the principal partial-wave
(s, p, d) character of the associated molecular orbitals, and the highest
occupied orbital in each cluster is indicated by the "Fermi level" (ε_F).
Since these clusters are intended to simulate the local interstitial bonding
configurations of isolated hydrogen atoms embedded in an otherwise perfect
bulk or surface lattice, the energy levels of the clusters containing hydrogen
have been shifted with respect to those of the corresponding hydrogen-
free clusters so that the respective Fermi levels line up. This approxima-
tion is based on the assumption that hydrogen chemisorption or absorption

in the dilute limit does not severely perturb the chemical potential of the metallic host and is supported by the observation from photoemission data that the work functions of crystalline nickel, palladium, and platinum change by no more than $\pm$ 0.2 eV with hydrogen chemisorption [17].

The electronic structure of each metal cluster shown in Fig. 4 is characterized by a manifold of closely spaced d-levels bracketed by s,p- or s,p,d-hybrid levels. This is similar to the results obtained for larger Ni, Pd, and Pt clusters, as described in Ref. [4], and analogous to the overlap of the "d-band" by the "s,p-like conduction band" in the respective bulk crystalline metals [27]. In each cluster, the Fermi level (ε_F) passes through the top of the d-band, just as in the bulk transition metals [27]. Although the calculated d-band width of each metal cluster is less than that of the corresponding bulk metal, the trend of increasing bandwidth and downward trend of the energy levels from Ni_4 to Pd_4 to Pt_4 is similar to the trends for the crystalline metals. Furthermore, the electronic structures of the Pd_4 and Pt_4 clusters are more nearly alike than those of the Ni_4 and Pd_4 or Ni_4 and Pt_4 clusters, consistent with the band structures of the corresponding crystalline metals. The deepest energy levels shown in Fig. 4 for Pd_4 and Pt_4 respectively, associated with cluster orbitals having the a_1 representation of the T_d point group and corresponding roughly to the Bloch band-structure states having the Γ_1 representation of the crystal space group, are predominantly d-like with a small amount of s,p-hybridization. In contrast, the deepest energy level for the Ni_4 cluster shown in Fig. 4, also associated with an a_1 molecular orbital and Γ_1 Bloch state, is predominantly s-like, but with significant d-orbital hybridization and some p-like character. These differences between the electronic structure of nickel aggregates and the electronic structures of palladium and platinum aggregates are crucial to understanding the differences in the photoemission

spectra for hydrogen chemisorbed on these metals [17], as well as the differ-
ences among these metals with respect to hydrogen solubility [24] and
catalytic reactivity [23].

According to the discussion presented in Section II of this paper, the
relative positions of the SCF-$X\alpha$ orbital energies for the Ni_4, Pd_4, and Pt_4
clusters with respect to the SCF-$X\alpha$ 1s-orbital energy for atomic hydrogen,
as shown in Fig. 4, are a measure of the relative orbital-electronegativity
and chemical-potential differences between these metal aggregates and
hydrogen. Thus the covalent bonding of atomic hydrogen at the cluster
interstices is governed principally by the proximity in energy (or electro-
negativity) and concomitant overlap of the symmetry-conserving [11] a_1
orbitals near the bottom of the Ni_4, Pd_4, and Pt_4 d-bands with the H 1s
orbital. The main result is the splitting off of a hydrogen-metal bonding
energy level of a_1 orbital symmetry from the bottom of the d-band of each
cluster, accompanied by much smaller level shifts within the d-manifolds,
as indicated in Fig. 4 by the orbital energies for the Ni_4H, Pd_4H, and Pt_4H
clusters and the connecting dashed lines. The metallic 4s-like component
of this a_1 orbital is largely responsible for the bonding of hydrogen to
the nickel aggregate, as indicated by the partial-wave decomposition of
the orbital. However, the contribution of the 3d-like component to the
bonding is not negligible, amounting to 35% of the Ni_4-H a_1 bonding orbital
charge. This result is inconsistent with the claims of other workers [28,29]
who, on the basis of theoretical studies of the interaction of hydrogen with
only one or two nickel atoms, find that the Ni 3d orbitals remain essentially
localized and atomic-like and therefore conclude that these orbitals do not
contribute to the chemisorption of hydrogen on nickel. In contrast to the
results for nickel, the metal d-orbital components almost exclusively dominate
the bonding of hydrogen to palladium and platinum aggregates, the contributions

of Pd 5s- and Pt 6s-like components amounting to only 15% and 12% for Pd_4H
and Pt_4H respectively. The covalent overlap of directed Pd d-orbitals with
the H 1s orbital is implicit in the contour map of the a_1 bonding orbital
shown in Fig. 5, plotted in the plane defined by the hydrogen atom and two
palladium atoms. These results underscore the danger of making general
conclusions about the dominance of s-orbitals over d-orbitals in determining
the chemisorption and catalytic reactivity of hydrogen on transition metals
exclusively on the basis of theoretical studies of first-row transition
metals, as has recently been done by some workers in the published litera-
ture [28,29]. The present findings are essentially unaltered for hydrogen
interacting with nickel, palladium, and platinum aggregates having other
cluster configurations large enough to realistically simulate the bulk and
surface electronic structures of these metals and small particles thereof.
For example, the partial-wave decompositions of the orbitals responsible
for the bonding of hydrogen at the octahedral interstices of six-atom clusters
are very similar to the results described above.

The most striking confirmation of these theoretical results is the
photoemission spectra recently measured by Demuth [17] for hydrogen chemi-
sorbed on the (111) faces of nickel, palladium, and platinum. For each metal,
the data clearly show a chemisorption-induced photoemission peak at an energy
slightly higher than the metal d-band photoemission peaks, suggestive of a
hydrogen-metal bonding state or "resonance" split off from the manifold of
d-orbitals as predicted in Fig. 4. On the basis of the intensity and width of
the chemisorption-induced photoemission peak as a function of incident photon
energy, Demuth [17] concludes that hydrogen chemisorption on Ni(111) occurs
primarily via the s-orbitals (with some d-orbital participation), whereas the
metal d-orbitals dominate hydrogen chemisorption on Pd(111) and Pt(111). This
interpretation is completely consistent with the partial-wave decomposition of

the hydrogen-metal bonding orbitals of a_1 symmetry described above. Further-
more, the chemisorption-induced spectral modification of d-band photoemission
from Pd(111) and Pt(111) surfaces [17] is explicable in terms of the calculated
shifts of d-manifold energy levels in going from Pd_4 to Pd_4H and from Pt_4 to
Pt_4H (Fig. 4). On the other hand, the uniform enhancement of the d-band photo-
emission from the Ni(111) surface upon hydrogen chemisorption is consistent
with the almost negligible shifts calculated for the d-orbital manifold in
going from Ni_4 to Ni_4H. The relative energies of the metal cluster d-orbital
manifolds with respect to the H 1s level indicated in Fig. 4, in conjunction
with the concept of orbital electronegativity, imply that a platinum aggregate
is somewhat of an electron acceptor with respect to atomic hydrogen, whereas
nickel and palladium aggregates are slight electron donors. This finding is
consistent with Demuth's [17] photoemission results for hydrogen chemisorption
on the surfaces of these metals, which show a slight decrease in the work
function of Pt(111) and slight increases in the work functions of Ni(111) and
Pd(111) upon hydrogen chemisorption. The close correspondence between the
theoretical results for hydrogen bonded to the interstices of tetrahedral Ni_4,
Pd_4, and Pt_4 clusters and the photoemission spectra for hydrogen chemisorbed
on Ni(111), Pd(111), and Pt(111) strongly supports our conjecture that such
chemisorption leads to incorporation of hydrogen atoms in the tetrahedral
interstices bounded by the (111) surfaces.

In regard to the well known fact that atomic hydrogen is more soluble
in palladium than in nickel or platinum [24], the almost perfect tuning of
the palladium cluster d-orbital electronegativities to the hydrogen 1s-orbital
electronegativity, as indicated in Fig. 4 by the relative positions of the
corresponding energy levels, suggests almost perfect covalency between
palladium, in aggregate form, and atomic hydrogen. In contrast, nickel and
platinum aggregates are respectively electropositive and electronegative
with respect to hydrogen. The strength of a heteronuclear chemical bond,

as originally described by Pauling [30], can be viewed as having covalent and ionic contributions in general. It is well known that the solubility of an impurity in a metal generally decreases with increasing electronegativity difference between solute and solvent, other factors such as atomic size remaining constant [31]. Thus the attainment of nearly zero net orbital electronegativity difference between palladium aggregates and atomic hydrogen, thereby minimizing ionic contributions to the bonding and optimizing $Pd(4d)$-$H(1s)$ covalency, is consistent with the higher solubility of hydrogen in palladium, as compared with nickel and platinum. The labile exchange of dissociatively chemisorbed hydrogen atoms between the surface and underlying interstices, making the metal a reservoir for atomic hydrogen, could facilitate the reactivity of hydrogen with other chemisorbed molecules, offering a possible explanation of why palladium is an order of magnitude more active in catalyzing hydrogenation reactions than nickel or platinum [32]. Although the metal-metal internuclear distances in the clusters have been constrained in the present studies to the values for the corresponding bulk crystalline metals, previous theoretical work on the cohesive energies of metal clusters has shown that the equilibrium internuclear distance decreases somewhat with decreasing number of atoms in the cluster [33]. The latter finding suggests that the size factor for small metal clusters is less favorable for interstitial hydrogen incorporation than larger particles or crystallites, thus providing a possible explanation of the observed reduction of hydrogen solubility with decreasing particle size [34].

Finally, the SCF-$X\alpha$-SW values for the relative 4s- and 3d-like partial-wave components of the Ni_4-H a_1 bonding orbital have already been used by Schönhammer [35] to parameterize an Anderson-type Hamiltonian for hydrogen chemisorption on nickel. From this, Schönhammer has calculated the adsorbate Green's function and the width of the chemisorption-induced photoemission peak, yielding a result in excellent agreement with the measurements of Demuth [17].

V. THE SURFACE REACTIVITY OF IRON

In the preceding two sections, we have attempted to show, applying the
concept of orbital electronegativity, how local coordination and composition
influence reactivity at transition-metal interfaces. In the present section,
by extending orbital electronegativity to spin orbitals as described in
Section II, we wish to show that local magnetic spin polarization can also
affect reactivity at transition-metal interfaces, using the surface reactivity
of representative iron clusters as an illustrative example. Of all the
transition metals, iron is one of the most reactive. In its pure crystalline
form, iron is readily oxidized. Among the first-row transition metals, iron
is the most active one for dissociating molecular nitrogen and is widely used
as a catalyst for the synthesis of ammonia [36,37]. Iron is also an excellent
catalyst for the Fischer-Tropsch synthesis of hydrocarbons from carbon
monoxide [23].

Spin-unrestricted SCF-Xα calculations have been carried out by C. Y.
Yang [38] for the electronic structures of 4-, 8-, 9-, 13-, and 15-atom
clusters of iron having tetrahedral and cubic geometries. All clusters show
significant spin polarization of the orbitals, with the 9- and 15-atom
clusters of bcc geometry exhibiting spin-polarized electronic structures that
are remarkably similar, to the extent that such comparisons can be made, to
the ferromagnetic band structure of bulk crystalline α-iron calculated by
Tawil and Callaway [39]. For the basis and justification of comparisons
between cluster electronic structures and crystalline band structures, which
have previously been made for copper, nickel, palladium, and platinum, the
reader should consult Ref. [4]. The SCF-Xα orbital energies for Fe_9 and
Fe_{15}, labeled according to the irreducible representations of the 0_h symmetry
group, are shown in Figs. 6 and 7, respectively. The Fermi level is indicated
by an arrow. The differences between the results for Fe_{15} and Fe_9 are mainly

quantitative, rather than qualitative, both clusters having the following
properties which are directly comparable with the band structures and measured
physical properties of ferromagnetic α-iron:

(1) The Fermi level of each cluster passes through the center of the manifold
of minority-spin d-levels, which is similar to the intersection of the
Fermi level with the minority-spin d-band of ferromagnetic α-iron [39].

(2) The combined density of levels for each cluster is qualitatively similar
to the density of states for α-iron deduced from photoemission spectra
[40]. In particular, the density of states for Fe_{15} is in better quanti-
tative agreement with the photoemission data [40] in regard to bandwidth
than is the density of states derived from band-structure calculations [39]
for crystalline iron, suggesting that the cluster spin orbitals are a
more realistic description of the initial states of photoemitted electrons
than are delocalized Bloch states.

(3) The magneton numbers per atom are 2.9 and 2.5 for Fe_9 and Fe_{15},
respectively, suggesting convergence to the 2.2 value characteristic
of ferromagnetic α-iron. The SCF-Xα results for successively smaller
iron clusters, such as Fe_8 and Fe_4, indicate convergence to larger values
of the magneton number approaching the atomic limit.

(4) The partial-wave decomposition of the Fe_9 and Fe_{15} cluster spin orbitals
indicates that the contribution of the 4s-like orbitals to spin polariza-
tion, although relatively small, is opposite in direction to the 3d-like
contribution, in good agreement with neutron diffraction measurements
[41].

(5) The spin densities along the [100] directions of the Fe_9 and Fe_{15} clusters,
corresponding to the direction of easy magnetization in crystalline α-
iron, are significantly larger than the spin densities along the [111]
directions, due to the greater concentration of spin density in the e_g

orbitals than in the t_{2g} orbitals. This result is in excellent quantitative agreement with neutron diffraction data [41] and provides a "real-space" interpretation of the latter.

(6) The transition from ferromagnetism to paramagnetism in crystalline α-iron around the Curie temperature can be explained within the framework of the Fe_{15} cluster model in terms of thermally induced long-range disordering of spin clusters and localized excitations of electrons within each cluster from the "spin-down" orbitals at the Fermi energy to the unoccupied $7t_{2g}\uparrow$ and $6e_g\uparrow$ orbitals lying just above the Fermi energy (see Fig. 7). The small increase of net magnetic moment of each cluster arising from the thermally induced depletion of minority-spin orbitals and population of majority-spin orbitals is consistent with neutron diffraction measurements in the vicinity of the Curie temperature. This is the first such explanation of a magnetic phase transition and lies beyond the scopes of conventional band theory and molecular-field theory.

A more detailed discussion of the relationships between these cluster calculations and the physical properties of crystalline α-iron will be the subject of a forthcoming paper [42], including a study of the effects of different boundary conditions on the clusters, a comparison of cluster and bulk densities of states, and calculations of the Heisenberg exchange integral and Curie temperature via Slater's [6] transition-state description of localized spin excitations. It is important here to underscore the fact that, despite the finite molecular nature of the clusters and the appearance of certain "surface-related" features of the cluster electronic structures (see below), the spin-polarized SCF-Xα results for the bcc Fe_9 and Fe_{15} clusters provide a remarkably successful model for the electronic and magnetic properties of crystalline α-iron. Similar theoretical studies have been made for cubo-octahedral Fe_{13} clusters representing fcc crystalline γ-iron [38]. The above

results, along with SCF-Xα cluster models (containing up to 44 atoms) for crystalline aluminum and chemisorption thereon [43], contradict the work of van Dyke [44] who concludes that such cluster calculations do not yield an adequately converged description of the properties of crystalline metals.

We can benefit by the large effective surfaces presented by the Fe_9 and Fe_{15} clusters to discuss the surface reactivity of iron, as has already been done for nickel, palladium, and platinum in Ref. [4] and in the preceding section of this paper. Among the manifolds of densely spaced d-orbital energies for the Fe_9 and Fe_{15} clusters (see Figs. 6 and 7) are levels which correspond to antibonding spin orbitals primarily localized on and spatially oriented away from the cluster boundaries or "surfaces," especially in the vicinity of the Fermi energy in the minority-spin d-manifold. Many of these spin orbitals have the proper spatial character for symmetry-conserving [11] overlap with the orbitals of certain reactant molecules. Moreover, the spin polarization raises the minority-spin orbitals to higher energies in comparison with the non-spin-polarized limit, effectively reducing the orbital electronegativity and facilitating overlap of the highest occupied iron surface spin orbitals with the lowest unoccupied or partially occupied orbitals of reactant molecules such as N_2, CO, and O_2. Since the latter orbitals are antibonding, overlap and effective electron flow from the iron surface spin orbitals to the unfilled reactant orbitals should promote molecular dissociation, the precursor to surface reactions of these molecules, such as ammonia synthesis, Fischer-Tropsch synthesis, and surface oxidation [23]. This argument is clarified by the direct comparison of representative Fe_9 cluster spin-orbital energies with the orbital energies of N_2, CO, and O_2 in Fig. 8, which is equivalent to comparing orbital electronegativities as discussed in Section II. Also included for comparison are the SCF-Xα orbital energies of a Pt_{13} cluster previously shown to exhibit many of the characteristics of the bulk and surface electronic

structures of crystalline platinum or small particles thereof [4]. In contrast to iron, there is no magnetic spin polarization in the platinum cluster, corresponding to the nonmagnetic character of bulk platinum, and the high density of d-orbitals around the Fermi level is poorly matched in energy and orbital electronegativity to the lowest unoccupied N_2 and CO orbitals. This result is consistent with the experimental fact that platinum is significantly less active than iron in promoting N_2 or CO dissociation and in catalyzing ammonia or Fischer-Tropsch synthesis [15,23]. Nickel is also magnetic, but the spin polarization of the d-orbitals is not large enough to yield a density of states around the Fermi level which is as well matched in energy and spin-orbital electronegativity to the lowest unoccupied orbitals of N_2 or CO as in the case of iron. This comparison is made in Fig. 9 and is consistent with the fact that nickel is a poor ammonia synthesis catalyst and is less active than iron in promoting Fischer-Tropsch synthesis [15,23]. With respect to the latter class of reactions, nickel is used mainly as a methanation catalyst [15]. The fact that iron is more readily oxidized than platinum is explained by the relative differences of the corresponding orbital energies and electronegativities with respect to the partially occupied antibonding π_g orbital of O_2, as shown in Fig. 8.

In an attempt to elucidate further the mechanism of ammonia synthesis on iron surfaces, Yang [38] has constructed cluster models for the so-called C7 active site, present on the (111) plane of bcc iron [37], and for a surface nitride of the type which may be formed after the rate-limiting step of N_2 dissociation. In Fig. 10, the $X\alpha$ spin-polarized orbital energies of an Fe_9N_6 cluster representing a face-centered surface nitride are compared with the orbital energies of the pure Fe_9 cluster. The distinguishing feature of the nitride electronic structure is a relatively narrow band of N 2p-like levels near the bottom of the Fe d-band, as indicated in Fig. 10, a result

which is confirmed by recently measured photoemission spectra for nitrogen chemisorbed on iron [40]. A detailed comparison of the Fe_9N_6 and Fe_9 electronic structures, along with the measured change in work function of iron upon nitrogen chemisorption [40], suggests some electronic charge transfer from iron to nitrogen in the formation of the surface nitride. The effective negative charge on the surface nitrogen atoms, together with the close matching of the nitride and H 1s orbital energies and electro-negativities, should facilitate protonation of the nitrogen atoms, the formation of N-H bonds, and ultimately ammonia synthesis.

A similar argument applied to the interaction of CO with iron leads one to conclude that a surface iron carbide, formed from the dissociation of CO on the iron surface, could facilitate protonation of the surface carbon atoms, the formation of C-H bonds, and the Fischer-Tropsch synthesis of hydrocarbons. There is already evidence that iron carbide will catalyze Fischer-Tropsch synthesis [23]. A theoretical study of this surface reaction is in progress at M.I.T., as are studies of the reactivity of N_2 on ruthenium and osmium, the second- and third-row transition metals which are good catalysts for ammonia synthesis.

BIBLIOGRAPHY

1. M. Boudart, in <u>Proceedings of the Robert A. Welch Foundation Conference on Chemical Research. XIV Solid State Chemistry</u>, edited by W. O. Milligan (The Robert A. Welch Foundation, Houston, Texas, 1970), p. 299.

2. J. H. Sinfelt, J. L. Carter, and D. J. C. Yates, J. Catal. <u>24</u>, 283 (1972).

3. J. C. Slater and K. H. Johnson, Phys. Rev. <u>B5</u>, 844 (1972); K. H. Johnson, in <u>Advances in Quantum Chemistry</u>, edited by P.-O. Löwdin (Academic, New York, 1973), Vol. 7, p. 143; K. H. Johnson and R. P. Messmer, J. Vac. Sci. Technol. <u>11</u>, 236 (1974); J. C. Slater and K. H. Johnson, Physics Today, October, 1974, p. 34; K. H. Johnson, in <u>Annual Review of Physical Chemistry</u>, edited by H. Eyring, C. J. Christensen, and H. S. Johnston (Annual Reviews, Palo Alto, California, 1975), Vol. 26, p. 39.

4. R. P. Messmer, S. K. Knudson, K. H. Johnson, J. B. Diamond, and C. Y. Yang, Phys. Rev. <u>B13</u>, 1396 (1976).

5. K. H. Johnson, in <u>Proceedings of the Second International Congress of Quantum Chemistry</u>, edited by B. Pullman and R. Parr (Reidel, Dordrecht, Holland, 1976), p. 317.

6. J. C. Slater, in <u>Advances in Quantum Chemistry</u>, Vol. 6, edited by P.-O. Löwdin (Academic, New York, 1972), p. 1; J. C. Slater, <u>The Self Consistent Field for Molecules and Solids</u>, Vol. 4 of <u>Quantum Theory of Molecules and Solids</u> (McGraw-Hill, New York, 1974).

7. J. Hinze, M. A. Whitehead, and H. H. Jaffe, J. Am. Chem. Soc. <u>85</u>, 148 (1963).

8. R. S. Mulliken, J. Chem. Phys. <u>46</u>, 497 (1949).

9. L. Pauling, J. Am. Chem. Soc. <u>54</u>, 3570 (1932).

10. K. Fukui, Bull. Chem. Soc. Japan <u>39</u>, 498 (1966); K. Fukui and H. Fujimoto, Bull. Chem. Soc. Japan <u>39</u>, 2116 (1966).

11. R. G. Woodward and R. Hoffmann, Accounts Chem. Res. 1, 17 (1968); The Conservation of Orbital Symmetry (Academic, New York, 1969).

12. R. G. Pearson, Theoret. Chim. Acta (Berlin) 16, 107 (1970); Accts. Chem. Res. 4, 152 (1971).

13. R. Ugo, Catal. Rev. Sci. Eng. 11, 225 (1975); R. Ugo, G. La Monica, F. Cariati, S. Cenini, and F. Conti, Inorg. Chim. Acta 4, 390 (1970).

14. G. A. Somorjai, in The Physical Basis for Heterogeneous Catalysis, edited by E. Drauglis and R. I. Jaffee (Plenum, New York, 1975), p. 395.

15. J. R. Anderson, The Structure of Metallic Catalysts (Academic, New York, 1975), p. 244.

16. R. P. Messmer, D. R. Salahub, K. H. Johnson, and C. Y. Yang, Chem. Phys. Lett. (submitted for publication).

17. J. E. Demuth, to be published and private communication.

18. L. Cassar, P. E. Eaton, and J. Halpern, J. Am. Chem. Soc. 92, 3515 (1970).

19. G. G. Eberhart and L. Vaska, J. Catal. 8, 183 (1967).

20. J. C. Slater and K. H. Johnson, Physics Today 27, 34 (1974).

21. R. P. Messmer, in The Physical Basis for Heterogeneous Catalysis, edited by E. Drauglis and R. I. Jaffee (Plenum, New York, 1975), p. 261.

22. C. W. Koeppl, J. Chem. Phys. 59, 3425 (1973), and references therein.

23. G. C. Bond, Catalysis by Metals (Academic, New York, 1962).

24. F. A. Lewis, in The Palladium/Hydrogen Systems (Academic, New York, 1967).

25. C. Y. Yang and S. Rabii, Phys. Rev. A12, 362 (1975); C. Y. Yang, Chem. Phys. Lett. 41, 588 (1976).

26. D. E. Eastman, J. K. Cashion, and A. C. Switendick, Phys. Rev. Lett. 27, 35 (1971).

27. See, for example, Electronic Density of States, edited by L. H. Bennett (National Bureau of Standards Spec. Pub. 323, Washington, D. C., 1971).

28. A. B. Kunz, M. P. Guse, and R. J. Blint, J. Phys. $\underline{B8}$, L358 (1975);
    R. J. Blint, A. B. Kunz, and M. P. Guse, Chem. Phys. Lett. $\underline{36}$, 191 (1975);
    A. B. Kunz, M. P. Guse, and R. J. Blint, in Electrocatalysis on Non-Metallic Surfaces, edited by A. D. Franklin (National Bureau of Standards, Spec. Pub. 455, Washington, D.C., 1976), p. 53.

29. C. F. Melius, Chem. Phys. Lett. $\underline{39}$, 287 (1976); C. F. Melius, J. W. Moskowitz, A. P. Mortola, M. B. Baille, and M. A. Ratner, Surf. Sci. $\underline{59}$, 279 (1976).

30. L. Pauling, The Nature of the Chemical Bond (Cornell University Press, Ithaca, N. Y., 1960), p. 80.

31. W. Hume-Rothery, The Structure of Metals and Alloys (institute of Metals, London, 1936).

32. G. C. A. Schuit and L. L. van Reijen, Adv. Catal. $\underline{10}$, 242 (1958).

33. J. G. Fripiat, K. T. Chow, M. Boudart, J. B. Diamond, and K. H. Johnson, J. Molec. Catal. $\underline{1}$, 59 (1975).

34. M. Boudart, Private communication.

35. K. Schönhammer, Chem. Phys. Lett. (in press); Int. J. Quantum Chem. $\underline{11S}$, 000 (1977), this volume.

36. P. H. Emmett, in The Physical Basis for Heterogeneous Catalysis, edited by E. Drauglis and R. I. Jaffee (Plenum, New York, 1975), p. 3.

37. M. Boudart, H. Topsøe, and J. A. Dumesic, in The Physical Basis for Heterogeneous Catalysis, edited by E. Drauglis and R. I. Jaffee (Plenum, New York, 1975), p. 337.

38. Chiang Y. Yang, Ph.D. Thesis, Department of Materials Science and Engineering, M.I.T. (in progress).

39. R. A. Tawil and J. Callaway, Phys. Rev. $\underline{B7}$, 4242 (1973).

40. F. Bozso, G. Ertl, M. Grunze, and M. Weiss, to be published.

41. C. G. Shull and Y. Yamada, J. Phys. Soc. Japan 17, Suppl. B-III, 1 (1962); C. G. Shull and H. A. Mook, Phys. Rev. 16, 184 (1966).

42. C. Y. Yang and K. H. Johnson, manuscript in preparation.

43. R. P. Messmer and D. R. Salahub, Int. J. Quantum Chem. 10S, 183 (1976); further work to be published and private communication.

44. J. P. Van Dyke, Bull. Am. Phys. Soc. 21, 232 (1976).

FIGURE CAPTIONS

Figure 1.   SCF-Xα orbital energies for coordinatively unsaturated transition-metal complexes representing low-coordination transition-metal sites and dissociative hydrogen chemisorption thereon. The highest occupied orbital is indicated by the "Fermi level" ε_F.

Figure 2.   Contour maps of the principal bonding and antibonding molecular-orbital wavefunctions corresponding to the orbital energies of the L_2MH_2 complex shown in Fig. 1.

Figure 3.   Possible reaction path for the hydrogenation of acetylene at a coordinatively unsaturated transition-metal site.

Figure 4.   Relativistic SCF-Xα orbital energies of tetrahedral Group-VIII transition-metal clusters with and without interstitial atomic hydrogen.

Figure 5.   Contour map for the a_1 bonding orbital of the Pd_4H cluster.

Figure 6.   Spin-polarized SCF-Xα orbital energies of a 9-atom bcc iron cluster.

Figure 7.   Spin-polarized SCF-Xα orbital energies of a 15-atom bcc iron cluster.

Figure 8.   Comparison of the SCF-Xα orbital energies of the Fe_9 and Pt_{13} clusters with those of the N_2, CO, and O_2 molecules.

Figure 9.   Comparison of the SCF-Xα orbital energies of the Fe_9 and Ni_{13} clusters with those of the N_2 and CO molecules.

Figure 10. Comparison of the SCF-Xα orbital energies of an Fe_9N_6 cluster representing a "surface iron nitride" with the orbital energies of an Fe_9 cluster representing pure iron and with the orbital energies of atomic hydrogen and nitrogen.
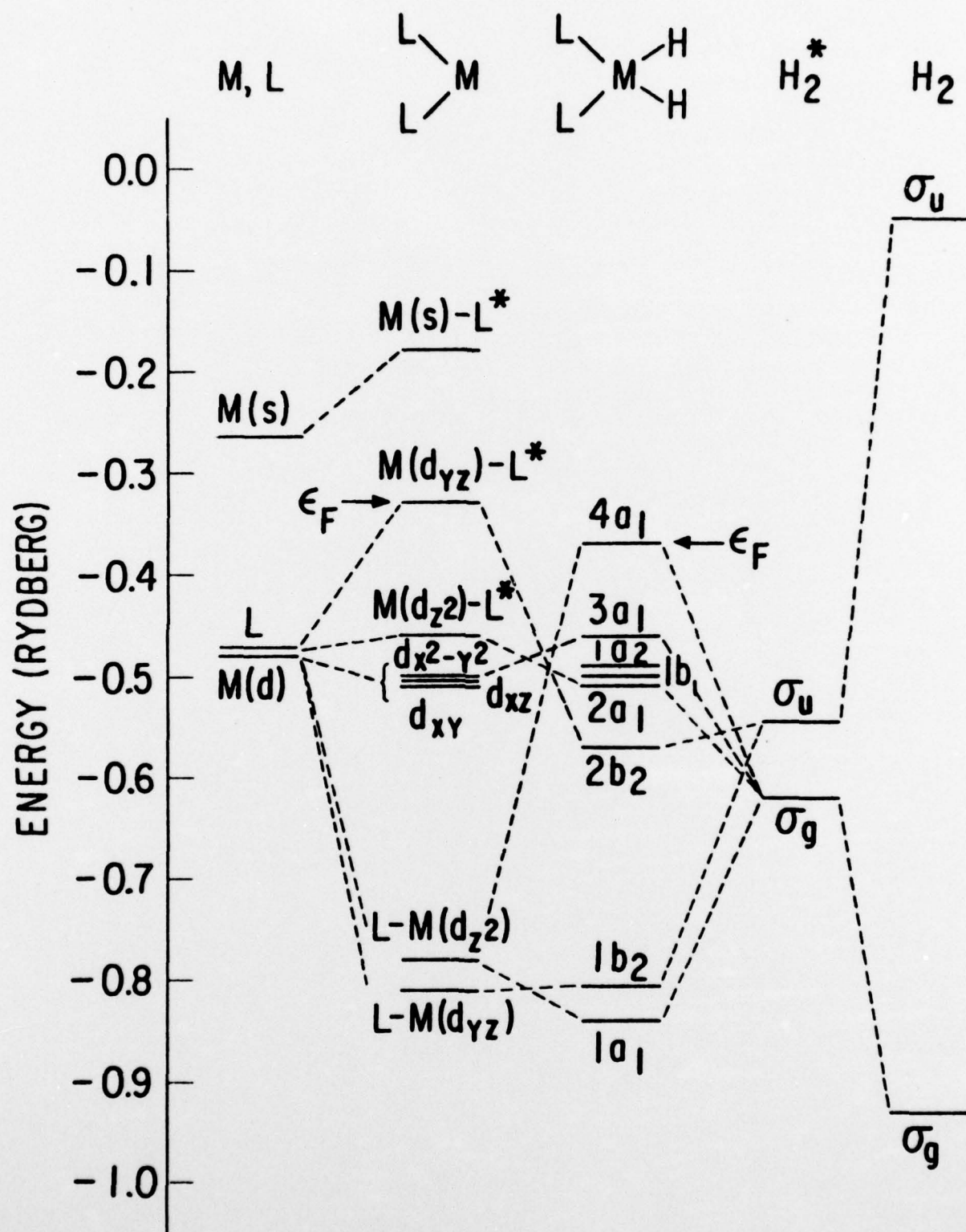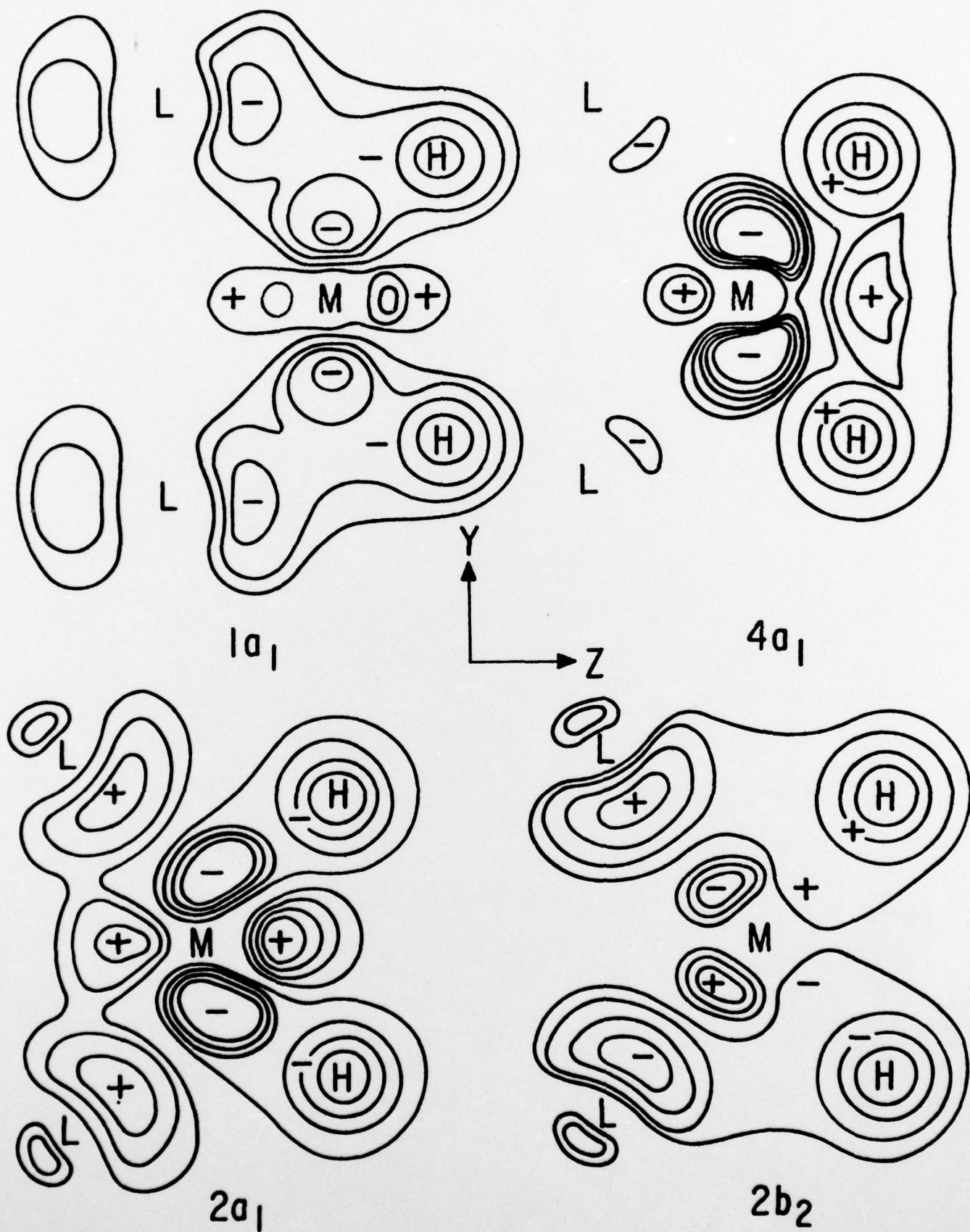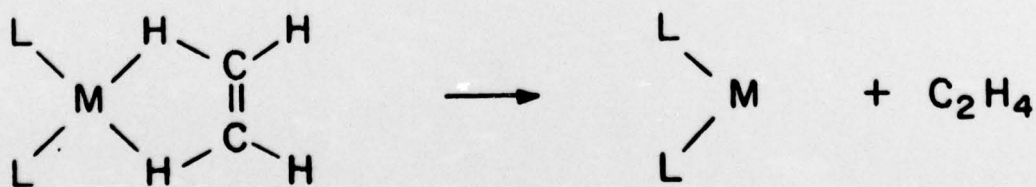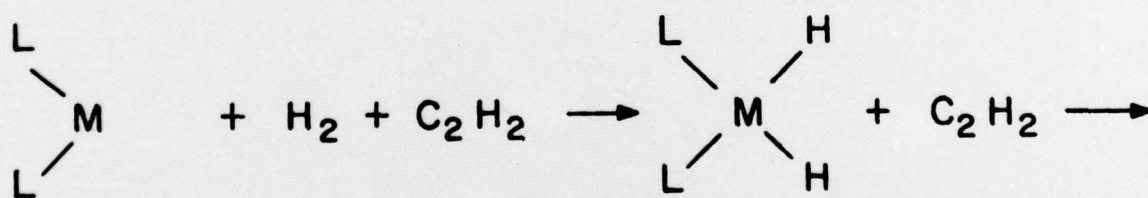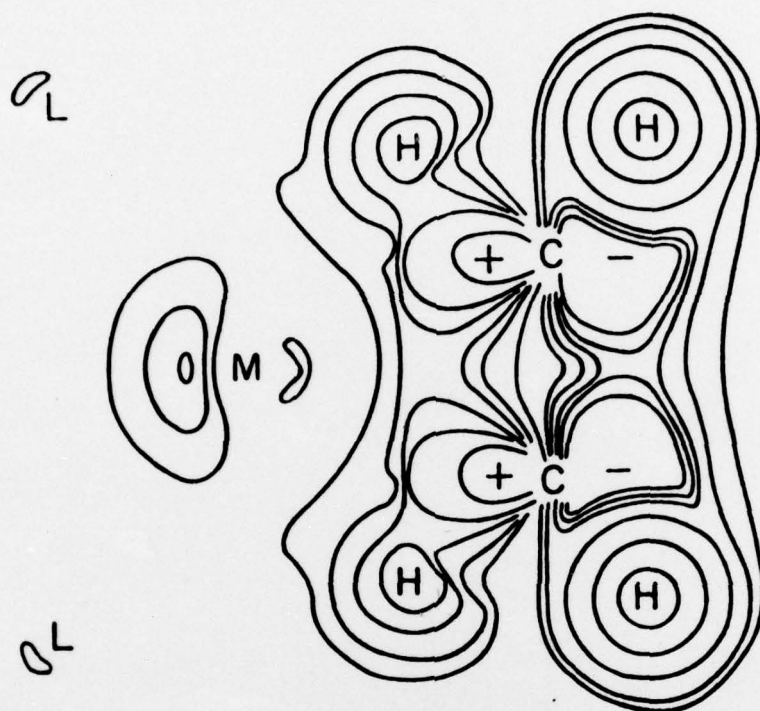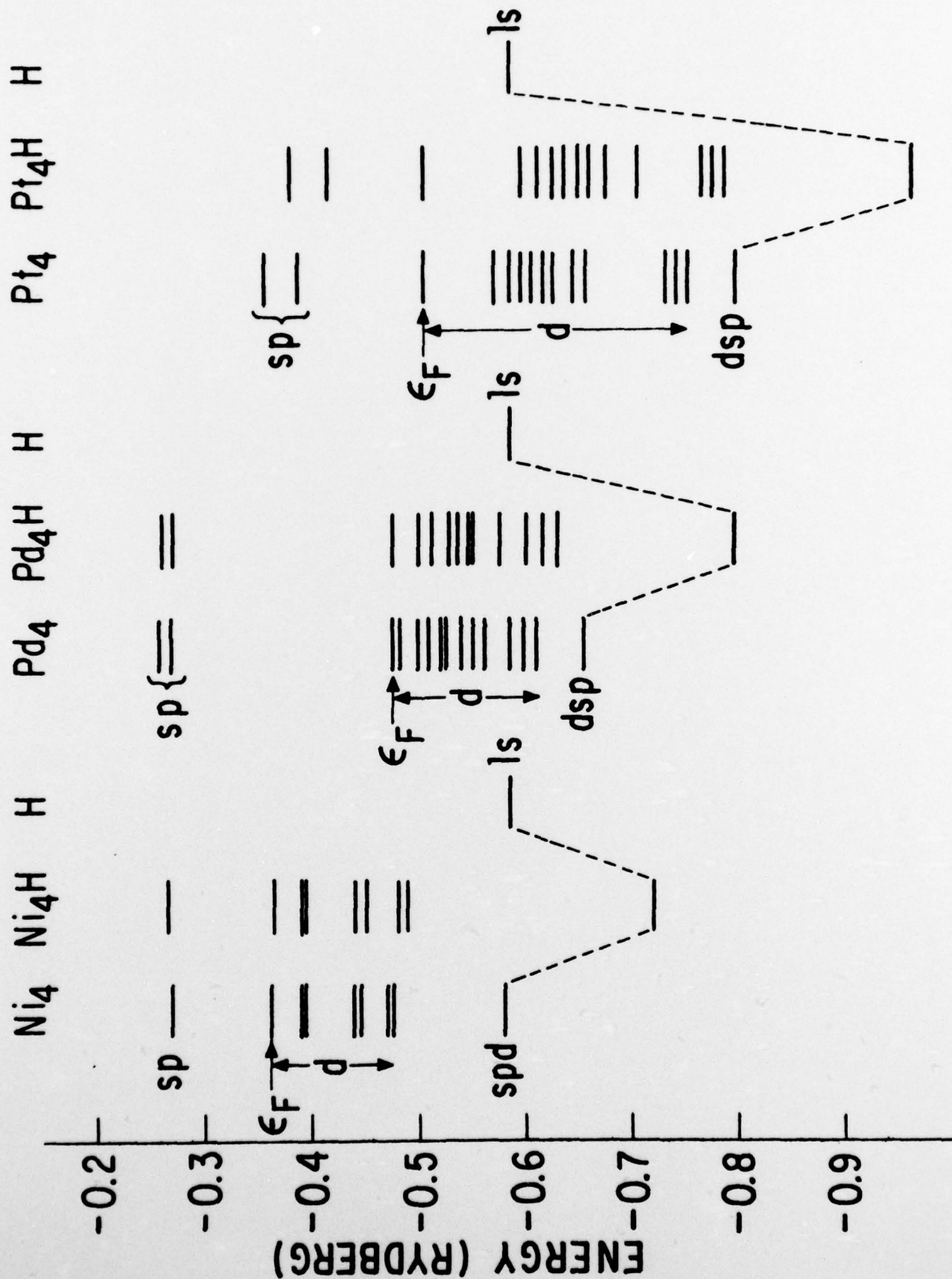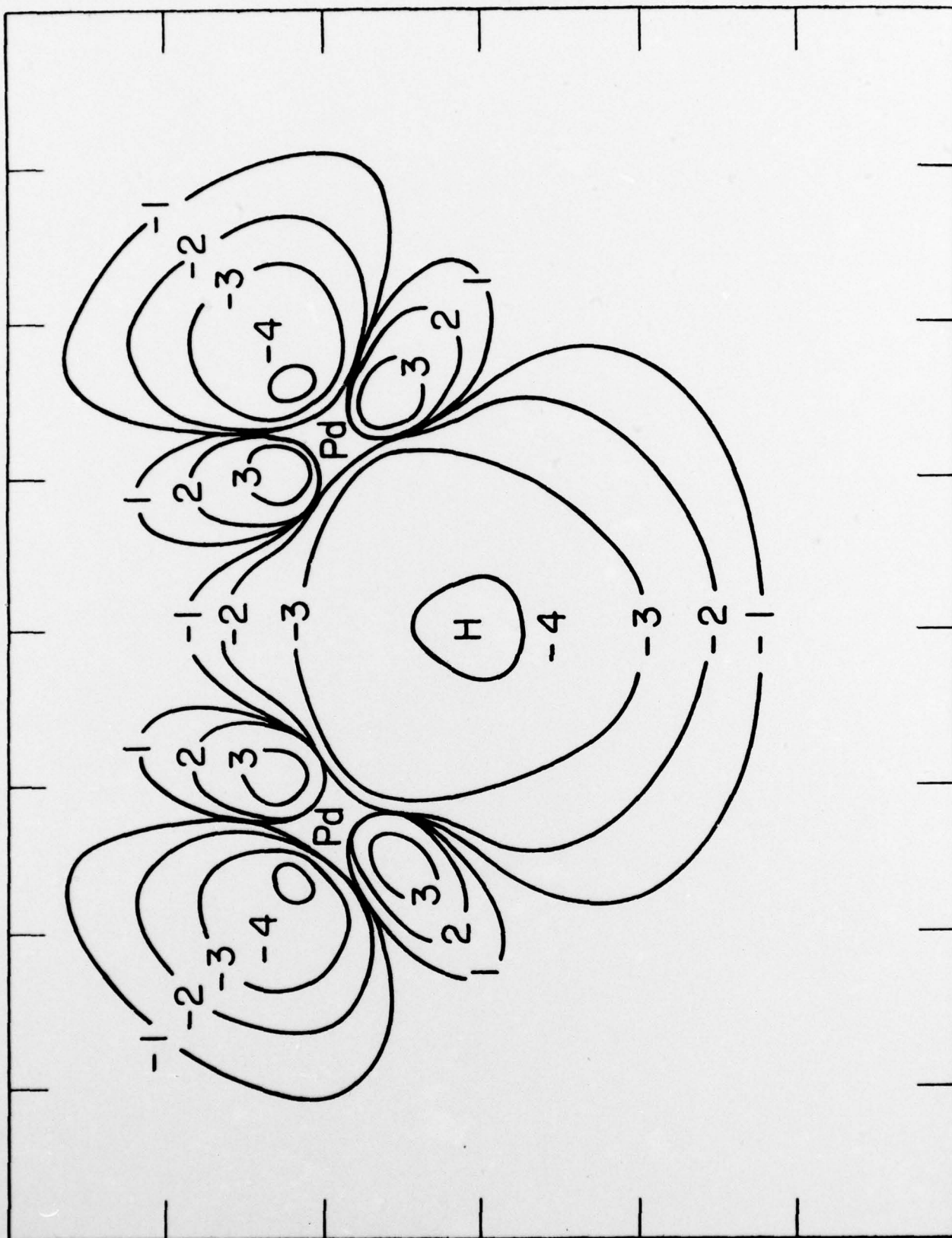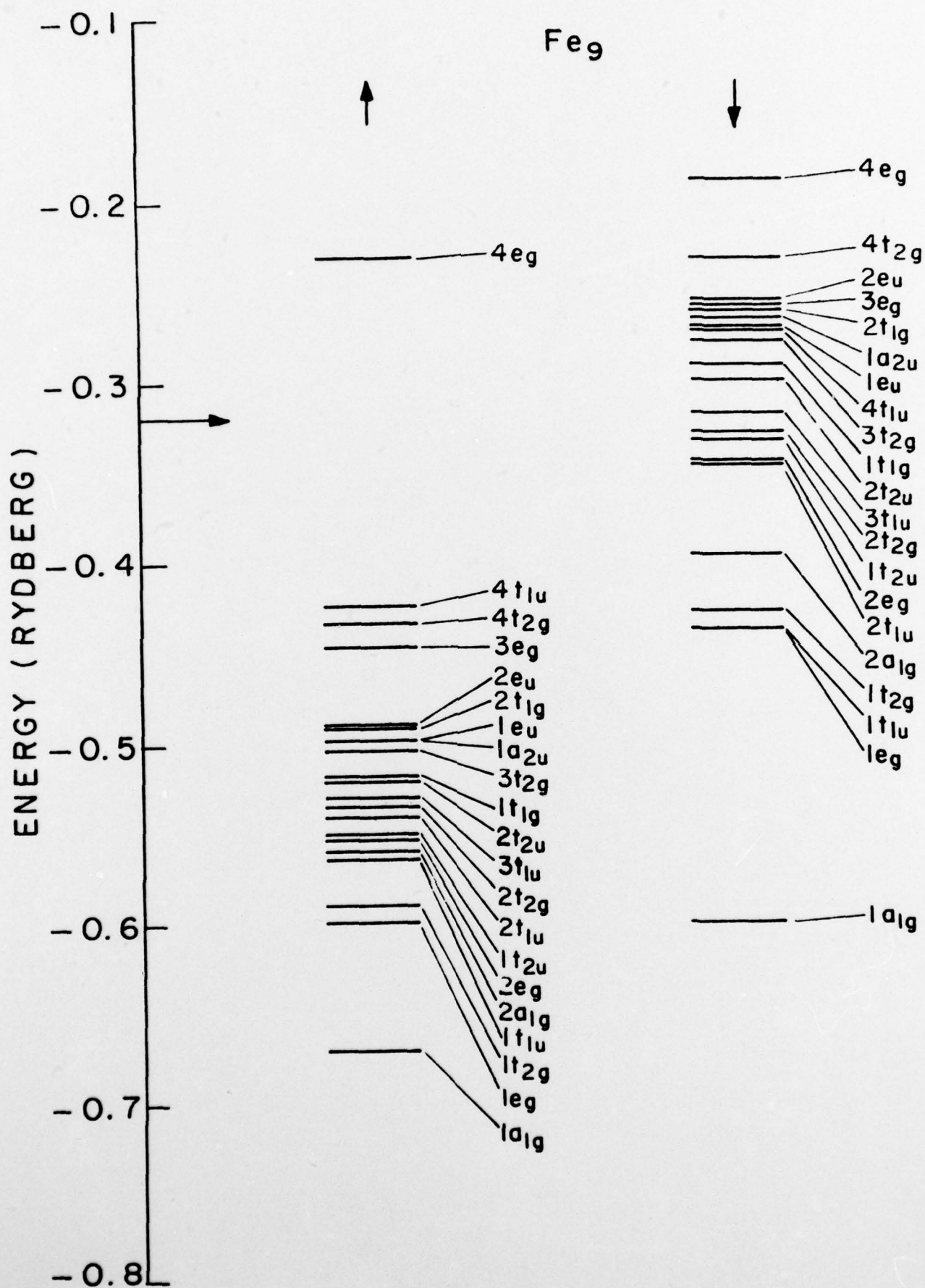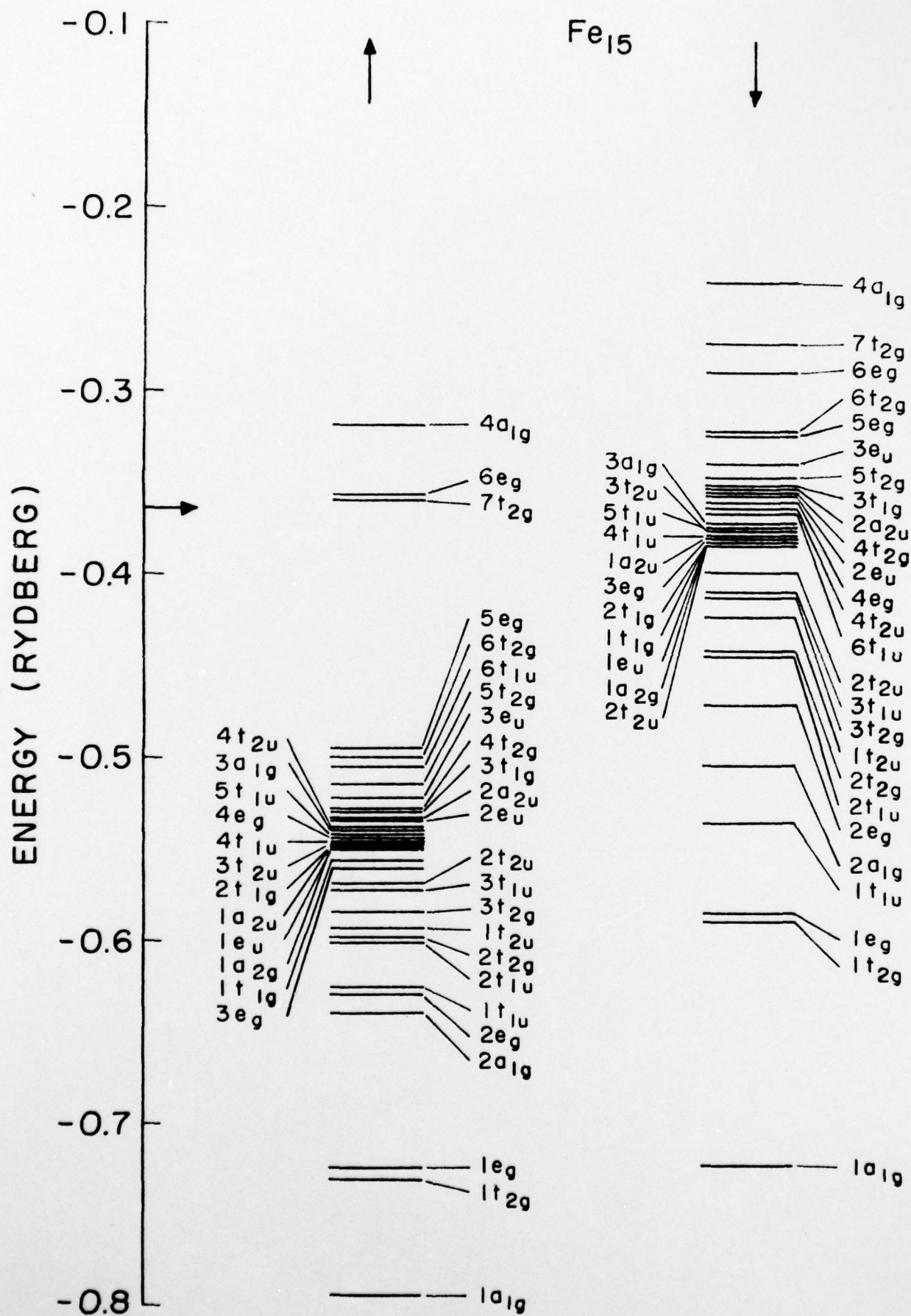
Figure 1

Figure 2

Figure 3

Figure 4

Figure 5

Figure 6

Figure 7

Figure 8

Figure 9

Figure 10